MNRAS **000**, 1–10 (2017) Preprint 16 March 2017 Compiled using MNRAS LATEX style file v3.0

The star formation environment of the FU Ori type star V582 Aur

M. Kun,[1⋆] E. Szegedi-Elek[1] and B. Reipurth[2]
[1] *Konkoly Observatory, Research Centre for Astronomy and Earth Sciences, Hungarian Academy of Sciences, H-1121 Budapest, Konkoly Thege út 15–17, Hungary*
[2] *Institute for Astronomy, University of Hawaii at Manoa, 640 N. Aohoku Place, Hilo, HI 96720, USA*

arXiv:1703.03674v2 [astro-ph.SR] 15 Mar 2017

16 March 2017

ABSTRACT

We have studied the environment of the FU Ori type star V582 Aur. Our aim is to explore the star-forming region associated with this young eruptive star. Using slitless spectroscopy we searched for Hα emission stars within a field of $11.5' \times 11.5'$, centred on V582 Aur. Based on UKIDSS and Spitzer Space Telescope data we further selected infrared-excess young stellar object candidates. In all, we identified 68 candidate low-mass young stars, 16 of which exhibited Hα emission in the slitless spectroscopic images. The colour–magnitude diagram of the selected objects, based on IPHAS data, suggests that they are low-mass pre-main-sequence stars associated with the Aur OB 1 association, located at a distance of 1.3 kpc from the Sun. The bright-rimmed globules in the local environment of V582 Aur probably belong to the dark cloud LDN 1516. Our results suggest that star formation in these globules might have been triggered by the radiation field of a few hot members of Aur OB 1. The bolometric luminosity of V582 Aur, based on archival photometric data and on the adopted distance, is 150–320 L$\odot$.

Key words: Stars: pre-main-sequence – Stars: formation – Stars: individual: V582 Aur – ISM: clouds – open clusters and associations: individual: Aur OB1

1 INTRODUCTION

FUors, named after their prototype FU Orionis, are young, low-mass stars undergoing powerful, long term (from decades to centuries) outbursts, powered by increased accretion (Hartmann & Kenyon 1996; Audard et al. 2014). During these events, FUors brighten up to 6 magnitudes over a few months, stay in a high state for decades, and as much as one tenth of the stellar mass may be added during these repeated outbursts. These young stars are members of star-forming regions both kinematically and spatially (Herbig 1966, 1977; Hartmann & Kenyon 1996). Studying the star forming environment of FUors is important for determining their distances and luminosities.

One of the less studied FU Ori type stars is V582 Aur (Samus 2009; Semkov et al. 2013). The brightening of V582 Aur was discovered by the amateur astronomer Anton Khruslov and the star was reported as a FUor candidate by Samus (2009). Semkov et al. (2013), based on photometric and spectroscopic observations of V582 Aur in its high state, confirmed its FUor nature. V582 Aur is projected on both the Aur OB 1 and Aur OB 2 associations, which are overlapping along the line of sight and situated at 1.32±0.1 and 2.8±0.27 kpc from the Sun, respectively (Humphreys 1978; Marco & Negueruela 2016). The region was included in several observational studies of the Galactic structure toward the anticentre (e.g. Marco & Negueruela 2016; Camargo, Bica & Bonatto 2013, and references therein). V582 Aur is projected within the area of the cluster CBB 9, identified by Camargo, Bonatto & Bica (2012), and on the periphery of the large dark cloud Lynds 1516 (Lynds 1962). No molecular cloud associated with Lynds 1516 was listed in Kawamura et al. (1998).

In order to explore the star formation environment of V582 Aur we searched for candidate young stellar objects in the region centred on V582 Aur. We utilized two striking characteristics of low- and intermediate-mass young stars, i. e. their specific near- and mid-infrared excesses, originating from circumstellar discs, and strong Hα emission, a signpost of mass accretion. We performed a search for new Hα emission line stars via slitless grism spectroscopy, using the University of Hawaii 2.2-m telescope, and used infrared data, available in the UKIDSS Galactic Plane Survey data base (Lucas et al. 2008) and in the *Spitzer* GLIMPSE360 Cata-

⋆ E-mail: kun@konkoly.hu

© 2017 The Authors

log and Archive. We further used optical photometric data, available in the IPHAS (Barentsen et al. 2014) DR2 Source Catalogue, to estimate distances and luminosities. We describe our observations and data reduction in Sect. 2. The procedures for young stellar object (YSO) identification in archival data are described in Sect. 3. The results are presented and conclusions are drawn in Sect. 4. We give a short summary in Sect. 5.

2 OBSERVATIONS AND DATA REDUCTION

We conducted a search for Hα emission stars in the vicinity of V582 Aur using the Wide Field Grism Spectrograph 2 (WFGS2) at the University of Hawaii 2.2-meter telescope on 2011 January 1. We used a 300 line mm^{-1} grism blazed at 6500 Å and providing a dispersion of 3.8 Å pixel^{-1} and a resolving power of 820. The Hα filter had a 500 Å passband, centred near 6515 Å. The detector for WFGS2 was a Tektronix 2048×2048 CCD, whose pixel size of 24 μm corresponded to 0.34 arcsec on the sky. The field of view was $11.5' \times 11.5'$, centred on V582 Aur. We took a short, 60 s exposure to identify the Hα line in the spectra of bright stars, and avoid saturation. Then we obtained two frames of 480 s exposure time, and co-added them to eliminate effects of the cosmic rays. Direct images of the same field were obtained through r' and i' filters before the spectroscopic exposures. One exposure was taken in each filter with integration time of 60 s. The steps of the data reduction were the same as described in detail in Szegedi-Elek et al. (2013).

We examined the co-added spectroscopic image visually to discover young stars showing the Hα line in emission, and found 16 emission-line objects in the observed region. We determined their equatorial coordinates by matching their positions, measured in the coadded grism image, with those of Two Micron All Sky Survey (Cutri et al. 2003) point sources in the direct images. All Hα emission sources had 2MASS counterparts within 1.4 arcseconds. We use 2MASS designations to identify the new Hα emission objects. The equivalent width of the Hα emission line EW(Hα) and its uncertainty were computed in the manner described by Szegedi-Elek et al. (2013). Due to the faint continuum and/or overlapping spectra we could measure EW(Hα) only in the spectra of nine stars. Table 1 lists the 2MASS designations and derived Hα equivalent widths of the emission objects detected in the WFGS2 images centred on V582 Aur. For comparison, we list EWs estimated from the IPHAS $r' - [\mathrm{H}\alpha]$ vs. $r' - i'$ colour–colour diagram (see Sect. 4.2) in column 5. To indicate the brightness of the stars r' magnitudes are listed in column 6 (see Sect. 3.4). The last column of Table 1 indicates the presence or absence of infrared excess over the 2.2–4.6 μm wavelength region (see Sects. 3.1 and 3.2).

3 YSO SELECTION FROM DATA ARCHIVES

3.1 UKIDSS

Pre-main-sequence stars, surrounded by protoplanetary discs, are clustered at specific regions in the $J-H$ vs. $H-K_s$ colour–colour diagram. Thus the colour–colour diagram is a useful tool to identify young stars. The region around V582 Aur was covered by the UKIDSS Galactic Plane Survey, some three magnitudes deeper than the 2MASS survey. We used the UKIDSS-DR6 Galactic Plane Survey data base (UGPS, Lucas et al. 2008), accessible in *VizieR*[1], to identify disc-bearing young stars in the area, identical with the field of view of our WFGS2 observations. Figure 1 presents the colour–colour diagram of the UKIDSS sources of the studied region. Small grey crosses show the distribution of all UKIDSS sources detected in each band, classified as stars with a probability pStar > 0.70, and having colour index uncertainties $\Delta(J-H) < 0.1$ and $\Delta(H-K_s) < 0.1$. Candidate YSOs in this diagram are sources whose errorbars are entirely to the right of the band of the reddened main sequence, bordered by the long-dashed lines. Reddened T Tauri stars occupy the grey area (Meyer, Calvet & Hillenbrand 1997). Taking into account the empirical nature of the T Tauri locus (dash-dotted line), we include a 0.1-mag wide band below this line into the T Tauri domain. Sources to the right of this band are candidate embedded protostars, whereas those below the locus of the unreddened T Tauri stars are somewhat uncertain in nature. Herbig Ae/Be stars are located in this part of the diagram (e.g. Manoj et al. 2006). These intermediate-mass pre-main-sequence stars are expected to be brighter than T Tauri stars of the same star-forming region. We checked the magnitudes of the K_s-band-excess sources below the unreddened T Tauri locus and found them to be among the faintest sources of the studied field. We ignore these sources, since their very red $H-K_s$ colour indices probably do not originate from protoplanetary discs. Red diamonds indicate the 42 selected candidate YSOs in Fig. 1. Additionally, twenty extended UKIDSS sources of the studied area, classified as probable galaxies, are located in the same region of the colour–colour plane. Extended sources, projected on a star-forming region, may be embedded protostars, whose appearance in the near-infrared is dominated by scattered light. We examined these sources in the UKIDSS and IPHAS images, and added six of them to the list of candidate YSOs. Black circles indicate these six extended sources in Figs. 1 and 3. The list of the UKIDSS-selected candidate YSOs is presented in Table 2. Ten Hα stars, detected in the WFGS2 images, have counterparts in this sample. V582 Aur itself is saturated in the UKIDSS images. Its 2MASS data, however, show it to be a K_s-band excess young star.

3.2 *Spitzer*

Our target field was also observed by the *Spitzer Space Telescope* (Werner et al. 2004) during its warm mission, as part of the GLIMPSE360 project (Churchwell et al. 2009). Observations were performed on 2010 May 4 with the Infrared Array Camera (IRAC, Fazio et al. 2004) at 3.6 and 4.5 μm (aors 38916864 and 38828288). We examined all sources within the $11.5' \times 11.5'$ environment of V582 Aur to search for additional young stars. We combined UKIDSS JHK_s magnitudes with *Spitzer* [3.6] and [4.5] magnitudes and applied the *Phase 2* selection criteria established by Gutermuth et al. (2009). This selection process includes dereddening of the colour indices of input stars onto the

[1] http://vizier.u-strasbg.fr/

Table 1. Hα emission stars identified during our *WFGS2* observations.

Name	2MASS Id	EW(Hα) (Å) WFGS2[a]	EW(Hα) (Å) IPHAS[b]	$r'_{\rm IPHAS}$ (mag)	IR excess
L1516-Ha 1	05252786+3457419	···	25	19.02	Y
L1516-Ha 2	05252963+3457551	8.0±2.5	25	17.78	Y
L1516-Ha 3	05253251+3457180	11.6±2.3	15	17.16	Y
L1516-Ha 4	05253272+3457107	13.7±2.2	50	16.51	Y
L1516-Ha 5	05253284+3455293	···	< 10	18.52	N
L1516-Ha 6	05253408+3457465	···	60	19.09	Y
L1516-Ha 7*	05254456+3450178	53.3±10.5	30	17.85	Y
L1516-Ha 8	05255203+3458081	6.8±0.7	80	18.36	Y
L1516-Ha 9*	05255439+3454391	37.3±4.2	50	17.45	Y
L1516-Ha 10	05255537+3454418	6.5±2.1	< 10	17.96	Y
L1516-Ha 11	05255688+3451442	46.6±5.6	100	16.96	Y
L1516-Ha 12	05260273+3451093	···	160	20.41	Y
L1516-Ha 13	05260711+3454260	···	< 10	18.00	Y
L1516-Ha 14	05261468+3450052	···	60	19.73	Y
L1516-Ha 15	05261637+3453332	15.4±7.7	< 10	17.72	Y
L1516-Ha 16	05261681+3454223	···	120	20.99	Y

[a]Measured in the slitless grism spectra. [b]Estimated from IPHAS photometry (Fig. 4). *Catalogued as Hα emission star in Witham et al. (2008) from IPHAS photometry.

YSO locus of the $J-H$ vs. $H-K_{\rm s}$ (or $H-K_{\rm s}$ vs. $[4.5]-[3.6]$ when J-band photometry is not available) diagram, and defines YSO colour criteria in the plane of the extinction-corrected $[K_{\rm s}-[3.6]]_0$ and $[[3.6]-[4.5]]_0$ colour indices. Fig. 2 shows the distribution of the point sources in the $[K_{\rm s}-[3.6]]_0$ vs. $[[3.6]-[4.5]]_0$ colour–colour diagram. To exclude dim extragalactic contaminants we applied $[3.6] < 14.0$ and $[4.5] < 14.0$ magnitude limits. Candidate YSOs are located in the upper right part of the diagram, bordered by the solid lines. Blue squares indicate the 48 candidate YSOs revealed by this selection. For comparison we plotted with red dots the candidate YSOs selected in the UKIDSS $J-H$ vs. $H-K_{\rm s}$ colour–colour diagram. The comparison shows that each previously selected object lies within the region assigned for YSOs, and a sizable part of them are fainter than 14 mag in the IRAC bands. We find 16 candidate YSOs not selected in the UKIDSS data. These stars are listed in Table 3. Their positions in the $JHK_{\rm s}$ colour–colour diagram are indicated by blue squares in Fig. 1. A 17th source, G172.7687-00.3577 (UGPS J052547.76+344950.9), classified as a probable UKIDSS galaxy, also fulfils the colour criteria. This very red object is projected on the edge of a dark cloud, therefore we include it in the list of candidate YSOs. Five Hα stars, detected in the WFGS2 images, have counterparts in this sample.

3.3 *WISE*

Marton et al. (2016a) performed a comprehensive all-sky search for candidate YSOs in the *AllWISE* data release. Six objects of their resulting catalogue (Marton et al. 2016b) can be found in our studied area, including V582 Aur itself. Three further among these candidates coincide with sources selected during the previous steps. These stars are marked in Tables 2 and 3. The remaining two objects are new candidate YSOs, listed in Marton et al.'s (2016a) catalogue as AllWISE J052614.87+345225.0 and AllWISE J052538.15+344805.0. The first source was classified as a probable galaxy (extended source) in the UKIDSS and IPHAS bands, therefore its nature is uncertain. The UKIDSS and *Spitzer* sources, coinciding in position with the second source within one arcsec, exhibit normal stellar colours, indicative of either an evolved (transitional) circumstellar disc, or two distinct sources.

3.4 IPHAS

The field we have studied was covered by the INT Photometric Hα Survey of the Northern Galactic Plane (IPHAS) survey (Drew et al. 2005). High-quality (S/N > 10) r' and i', and narrow-band Hα magnitudes are available for more than 800 stars of the studied $11.5' \times 11.5'$ region in the IPHAS DR2 Source Catalogue (Barentsen et al. 2014). These data are suitable for selecting further candidate YSOs (see Barentsen et al. 2011). Two of our 16 Hα emission stars appear in the first catalogue of Hα emission objects based on the IPHAS survey (Witham et al. 2008), containing stars brighter than $r' = 19.5$ mag. r', i', and Hα magnitudes are available for 35 of our candidate YSOs. We use these data to examine the Hα emission properties of the stars selected by infrared excesses, and establish the distance of the group of candidate YSOs around V582 Aur.

4 RESULTS

4.1 Surface distribution of candidate YSOs around V582 Aur

Figure 3 shows the surface distribution of the selected candidate young stars, overplotted on the IPHAS narrow-band Hα image of the studied $11.5' \times 11.5'$ region. The underlying Hα image reveals that V582 Aur and several candidate young stars are projected on bright-rimmed dark clouds.

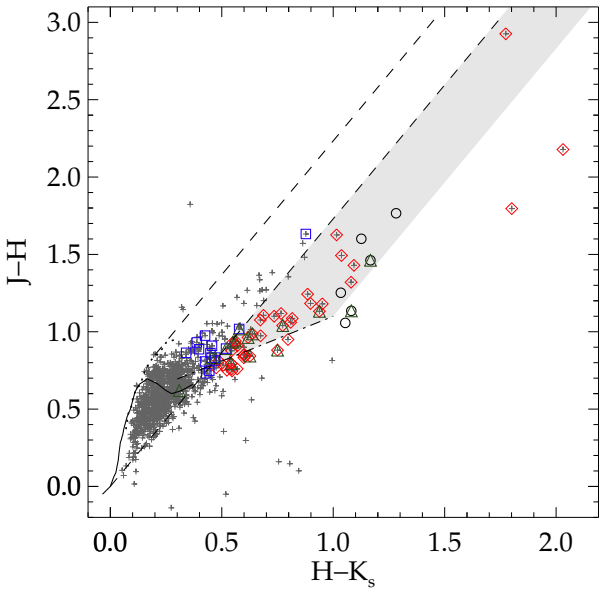

Figure 1. $J-H$ vs. $H-K_s$ colour–colour diagram of UKIDSS sources in a field of $11.5' \times 11.5'$, centred on V582 Aur. Small grey crosses indicate all stars having $\Delta(J-H) < 0.1$ and $\Delta(H-K_s) < 0.1$ in the UGPS catalogue. Red diamonds mark the candidate YSOs selected out of this sample. Green triangles show the Hα emission stars identified in the WFGS2 images. Black circles show the extended UKIDSS sources considered as candidate YSOs. The black solid curve shows the colours of the zero-age main sequence, and dotted line is the giant branch. The dash-dotted line is the locus of unreddened T Tauri stars (Meyer et al. 1997). The long-dashed lines delimit the area occupied by reddened normal stellar photospheric colours (Cardelli, Clayton & Mathis 1989). The grey shaded band indicates the area occupied by reddened K_s-band excess pre-main-sequence stars. For comparison, we plotted with blue squares candidate disc-bearing stars revealed by their 3.6 and 4.5-μm excess emission only.

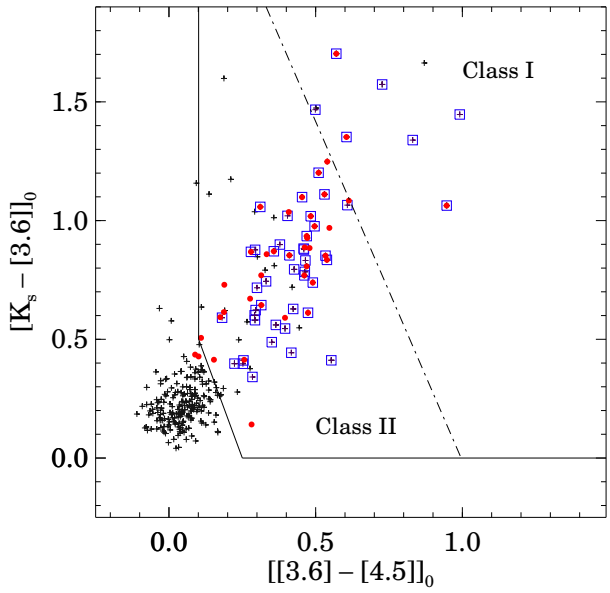

Figure 2. $[K_s-[3.6]]_0$ vs. $[[3.6]-[4.5]_0]$ colour–colour diagram of all *Spitzer* sources associated with UKIDSS sources and brighter than [3.6] = 14.0 mag and [4.5] = 14.0 mag in the $11.5' \times 11.5'$ area centred on V582 Aur. Solid lines delimit the region occupied by candidate YSOs, and the dash-dotted line separates Class I protostars from Class II pre-main-sequence stars according to Gutermuth et al.'s (2009) *Phase 2* method. Blue squares indicate candidate YSOs identified in this diagram, and red dots correspond to the sources selected by their K_s-band excess.

Striking features of the image are the elephant-trunk-like globule near the eastern edge, and the compact group of candidate YSOs clustered at the north-western corner. The dotted circle indicates the catalogued position of the CBB 9 cluster, identified by Camargo et al. (2012), and the dashed circle marks the position of the FSR 775 open cluster candidate, identified by Froebrich, Scholz & Raftery (2007) using 2MASS data, and rejected later as a real cluster by detailed structure studies by Camargo et al. (2012). The distribution of fainter UKIDSS and *Spitzer* sources suggest a remarkable clustering of candidate T Tauri stars projected near the centre of FSR 775. Some 40 per cent of the candidate YSOs can be found within 2 arcmin to the centre of FSR 775. Study of the radial profile of this group, however, is beyond the scope of the present paper. Our candidate young stars and V582 Aur itself are projected within these overlapping clusters. The B1 V type star HD 281147 (Marco & Negueruela 2016), mentioned by Camargo et al. (2012) as a possible member of CBB 9 is also labelled.

4.2 The nature of candidate YSOs associated with V582 Aur

All but one of the Hα emission stars detected by the WFGS2 exhibit infrared excesses characteristic of classical T Tauri stars. L1615-Ha 5 has no excess flux in the wavelength region covered by the UGPS and *Spitzer* GLIMPSE observations. Its low-quality *AllWISE* fluxes do not exclude excess emission at longer wavelengths. Its nature is thus uncertain: it may be either a pre-main-sequence star with evolved (transitional) disc, or weak-line T Tauri or M-type main sequence star with Hα emission. Another Hα source of uncertain nature is L1516-Ha 1, whose associated UKIDSS source was classified as a galaxy.

The $r'-[\mathrm{H}\alpha]$ vs. $r'-i'$ colour–colour diagram allows us to estimate the EW of the Hα emission line of the studied stars (Barentsen et al. 2011). Figure 4 shows this diagram for the 35 candidate YSOs detected in each IPHAS band. Synthetic colours of main sequence stars and Hα emission objects are taken from Barentsen et al.'s (2011) Table A1. The thick solid line indicates the normal main sequence, and thin solid lines show the main sequence colours modified by Hα emission. Each colour was reddened to E(B−V) = 0.40 mag, the lower limit of the foreground reddening towards the line of sight of V582 Aur (Green et al. 2015). It can be seen that not all of our candidate YSOs appear as Hα emission stars in this diagram. Nearly half of them (15 objects), including five of the WFGS2-detected Hα emission stars are scattered around the main sequence, below the line

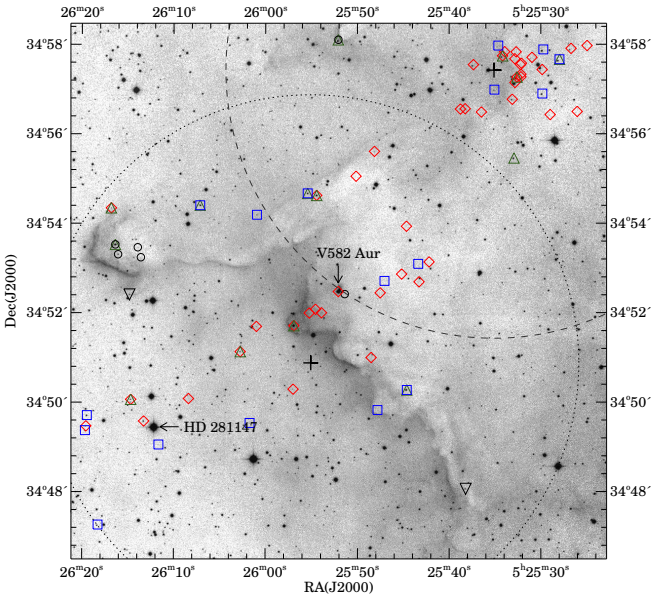

Figure 3. Candidate young stars identified during the present survey, overplotted on the IPHAS narrow-band Hα image. Green triangles represent Hα emission stars, red diamonds mark UKIDSS-selected sources, and blue squares indicate candidate pre-main-sequence stars exhibiting excess emission only in the *Spitzer* data. Small black circles indicate extended UKIDSS sources considered as candidate YSOs. Inverted triangles show the *AllWISE* sources listed in Marton et al.'s (2016a) catalogue of candidate YSOs. The large dotted circle indicates the position of the CBB 9 cluster, and the dashed circle marks the position and radius of the FSR 775 open cluster candidate. Crosses show the catalogued positions of the cluster centres.

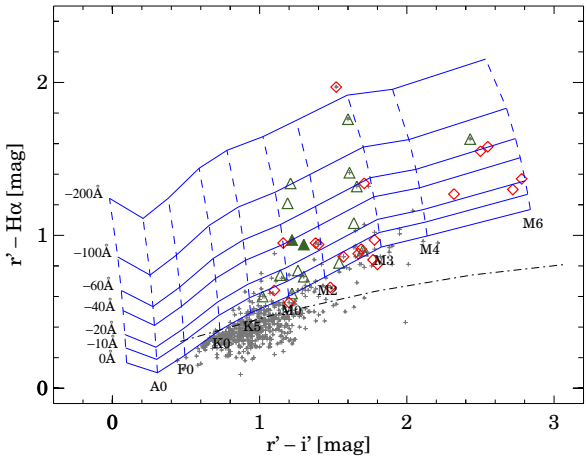

Figure 4. $r' - [\mathrm{H}\alpha]$ vs. $r' - i'$ colour–colour diagram of 35 candidate YSOs within the $11.5' \times 11.5'$ box around V582 Aur. Triangles indicate Hα emission stars identified in our WFGS2 images, and diamonds mark infrared-excess stars. Filled triangles mark the stars included in the IPHAS emission star catalogue (Witham et al. 2008). Small grey crosses show the colour distribution of the IPHAS sources with $S/N > 10$ in each band within the same area. Simulated colours of main sequence stars with Hα emission, computed by Barentsen et al. (2011) are indicated by the solid blue lines for $E(B-V) = 0.40$, the lower limit of foreground reddening towards the line of sight of V582 Aur. Dashed blue lines show the colour variations of the spectral types indicated at the lower ends, due to increasing EW(Hα). Dash-dotted line shows the reddening path of a K0 type star between $0 \leq E(B-V) \leq 4$.

corresponding to EW(Hα)=−10 Å. All of these stars, except L1615-Ha 5, have CTTS-like infrared excesses. Their positions may result from their significantly higher extinctions, or they may be variable classical T Tauri stars with temporarily low accretion activities. Figures 4 and 6 (Sect. 4.3) suggest that the L1516-Ha objects with weak Hα emission line are bluer and brighter on the average than the whole sample of the candidate YSOs. These properties suggest reddened G and early K type T Tauri stars, in which accretion may result in EW(Hα) below the −10 Å threshold (Barrado y Navascués & Martín 2003).

Figures 1 and 2 suggest that a few selected sources may be Class I protostars (Lada 1991). To confirm their nature we looked for mid- and far-infrared counterparts in the AllWISE, Akari IRC and Akari FIS data. Spectral energy distributions (SED) for three candidate protostars are displayed in Fig. 5. UGPS J052547.76+344950.9 is a faint, red source not detected in the UKIDSS J band. Its 22-μm flux indicates a Class I protostar. UGPS J052552.02+345808.2 is projected near the bright rim of a small cometary globule at the northern edge of the region. It is included in the catalogue of WISE YSO Candidates (Marton et al. 2016b). Its SED suggests a flat-spectrum object. UGPS J052616.37+345333.2 (L1516-Ha 15) is situated near the centre of the elephant-trunk-like cometary globule. Its SED suggests a Class I YSO. Another nearby candidate Class I YSO, UGPS J052616.07+345320.0, may contribute to the Akari FIS fluxes.

4.3 Colour–magnitude diagram: the distance of V582 Aur

When plotting the r' vs. $r' - i'$ colour–magnitude diagram one has to keep in mind that r' magnitudes may be modified by the presence of the Hα emission line within the r' band (Drew et al. 2005; Barentsen et al. 2011). We applied the correction to the r' magnitudes following Barentsen et al. (2011), and plotted the r' vs. $r' - i'$ colour–magnitude diagram of the candidate YSOs in Fig. 6. We compare their distribution with semi-empirical pre-main-sequence isochrones presented by Bell et al. (2014) for the IPHAS bands, based on the Pisa pre-main sequence tracks and isochrones (Tognelli et al. 2011) and BT-Settl (Baraffe et al. 2015, and references therein) atmosphere models. Isochrones bracketing from 10^6 to 2×10^7-year encompasses almost all disc-bearing pre-main-sequence stars, therefore we plotted in Fig. 6 isochrones for the distances and foreground extinctions of both Aur OB 1 and Aur OB 2. Foreground reddenings of $E(B-V) = 0.40$ mag and $E(B-V) = 0.90$ mag were adopted for Aur OB 1 and Aur OB 2, respectively (Green et al. 2015).

Most of the candidate YSOs in this diagram are widely scattered between the isochrones plotted for the distance and foreground extinction of Aur OB 1, and above or along the

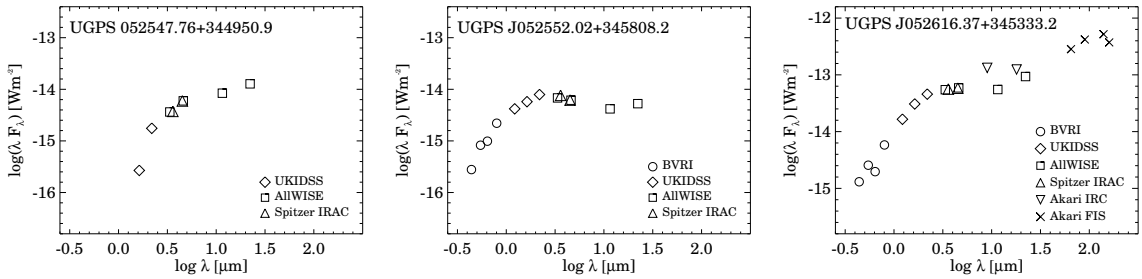

Figure 5. Spectral energy distributions of three candidate protostars in the environment of V582 Aur. Optical data are from the NOMAD Catalog and IPHAS.

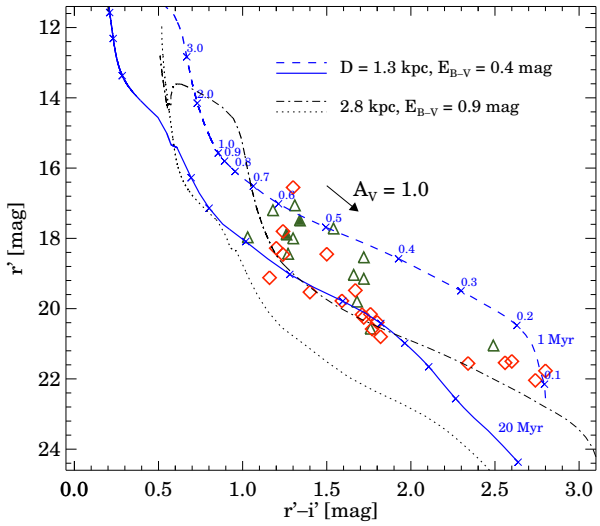

Figure 6. r' vs. $r'-i'$ colour–magnitude diagram of the 35 candidate YSOs detected by IPHAS. Symbols are same as in Fig. 4. 1 and 20-Myr isochrones (Bell et al. 2014) are drawn for the distances and foreground extinctions of Aur OB 1 (blue) and Aur OB 2 (black). Stellar masses between 0.1 and 3.0 $M_\odot$ are marked along the isochrones and labelled along the 1-Myr line.

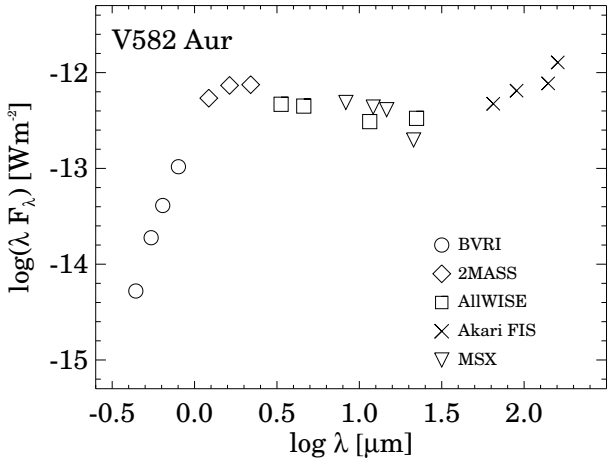

Figure 7. Spectral energy distribution of V582 Aur, based on archival data. *BVRI* data are averaged from Semkov et al.'s (2013) light curves.

1-Myr isochrone of Aur OB2. Taking individual extinctions into consideration would modify this distribution so that positions of the stars reddened by $E(B-V) > 0.40$ mag would move toward slightly younger isochrones and higher masses. The colour–magnitude diagram suggests the conclusion that the star-forming region around V582 Aur is probably associated with Aur OB1, located at 1.32 kpc from the Sun (Humphreys 1978).

4.4 Bolometric luminosity of V582 Aur

Our results suggest that the FUor V582 Aur is a member of a group of young low-mass stars, situated at a distance of 1.32 kpc from the Sun. The adopted distance allows us to estimate the luminosity of this outbursting young star. The SED of V582 Aur, constructed from archival data, is displayed in Fig. 7. The far-infrared source Akari FIS 0525509+345227, associated with V582 Aur in the Akari FIS YSO Catalogue of Tóth et al. (2014), is separated by 13.5″ from the star. Although this separation is smaller than the half-maximum radius of the point-spread function of the FIS (Arimatsu et al. 2014), unresolved nearby sources may contribute to the far-infrared fluxes. We integrated the SED to obtain the bolometric luminosity of V582 Aur, after correcting the fluxes for a foreground extinction $A_V = 1.53$ mag, taken from the IPHAS 3D extinction map of the Northern Galactic Plane (http://www.iphas.org/extinction/), and using Cardelli et al.'s (1989) extinction law. We obtained $L_{bol} = 324\,L_\odot$ with the FIS data included, and $L_{bol} = 146\,L_\odot$ without the far-infrared part of the SED. These values are typical for FUor outburst luminosities (Audard et al. 2014).

4.5 Connection of the new star-forming region with Aur OB 1

The colour–magnitude diagram of the candidate YSOs around V582 Aur suggests that their associated cometary globules and bright-rimmed dark clouds (Fig. 3) are lo-

cated within the volume of the Aur OB 1 associaton. The bright rims indicate interaction of the clouds with hot stars of the association. Aur OB 1 is defined by a few O and early B type stars (Humphreys 1978), and the 20-Myr old open cluster NGC 1960 (Reipurth & Yan 2008). Straižys, Drew & Laugalys (2010) established that the dark cloud LDN 1525 (TGU 1192), located some 2 degrees north-east from our studied area and associated with the H II region Sh2-235, is situated at 1.3 kpc from the Sun, within the volume occupied by Aur OB 1. Several signposts of on-going star formation were identified in the region of Sh2-235 (Dewangan et al. 2016, and references therein), which may be a possible young subsystem of Aur OB 1. The complex of bright-rimmed clouds, associated with V582 Aur, may represent another region of active star formation within the volume of Aur OB 1.

To find the possible ionizing stars we examined the wide-field environment of V582 Aur. Figure 8 presents a $2^\circ \times 2^\circ$ three-color image, centred on V582 Aur, and composed of the Digitized Sky Survey 2 blue (blue), *WISE* 12 μm (green), and *WISE* 22 μm (red) images. The image suggests that the cometary-shaped clouds at the centre are located on the south-eastern boundary of a large complex of clouds, including LDN 1516, and are apparently exposed to disruptive effects from the south-eastern direction. Two luminous members of Aur OB 1 from Humphreys' (1978) list are found within the area of the image. HD 35633 is a B0.5 IV type star, located at an angular distance of 0.51 deg from V582 Aur, corresponding to an 11.8 pc projected separation at 1.32 kpc. HD 35653 is a B0.5 V type star, at a projected distance of some 23 pc from V582 Aur. The ultraviolet radiation of these stars may ionize and compress the clouds. The spectacular H II region Sh2-234 is a background object at 2.8 kpc from the Sun. Spectroscopic and photometric data, available for the B1 V type star HD 281147 (see Fig. 3) in *VizieR*, suggest that this star is also a background object.

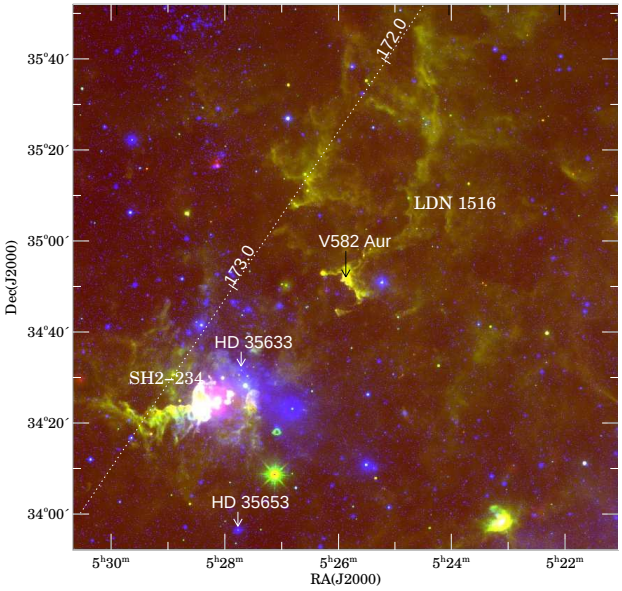

Figure 8. Three-colour image of the $2^\circ \times 2^\circ$ environment of V582 Aur, composed from the DSS2b (blue), *WISE* 12 μm (green), and *WISE* 22 μm (red) images. The newly identified bright-rimmed clouds can be seen in the middle of the image. The possible exciting stars are labelled. The dotted line shows the Galactic equator.

5 SUMMARY

We have investigated the star-forming environment of the less studied FUor V582 Aur. Based on Hα emission detected in slitless spectra and infrared excesses revealed by UKIDSS, *Spitzer*, and *WISE* archival data we identified 68 candidate low-mass young stars in the $11.5' \times 11.5'$ area centred on V582 Aur, among them two bona fide low-mass protostars. An optical colour–magnitude diagram of 35 members of the group, compared with pre-main-sequence evolutionary models, suggests that they represent a new, active star-forming subsystem of the Auriga OB 1 association, located at a distance of 1.32 kpc from the Sun. The narrow-band Hα image of the region, available in the IPHAS archive, reveals a system of bright-rimmed, cometary clouds associated with the newly identified young stars. Our results suggest that star formation in these clouds might have been triggered by the radiation field of a few hot members of Aur OB 1. The bolometric luminosity of V582 Aur, based on archival photometric data and on the adopted distance, is $146 \lesssim L_{\rm bol}/L_\odot \lesssim 324$.

ACKNOWLEDGEMENTS

This research is based on observations with the 2.2-m telescope of the University of Hawaii. We thank Colin Aspin and Mark Willman for their interest and support. We are grateful to Ágnes Kóspál for careful reading of the manuscript. This paper makes use of data obtained as part of the INT Photometric Hα Survey of the Northern Galactic Plane (IPHAS, www.iphas.org) carried out at the Isaac Newton Telescope (INT). The INT is operated on the island of La Palma by the Isaac Newton Group in the Spanish Observatorio del Roque de los Muchachos of the Instituto de Astrofisica de Canarias. All IPHAS data are processed by the Cambridge Astronomical Survey Unit, at the Institute of Astronomy in Cambridge. The bandmerged DR2 catalogue was assembled at the Centre for Astrophysics Research, University of Hertfordshire, supported by STFC grant ST/J001333/1. This work also makes use of observations made with the *Spitzer Space Telescope*, which is operated by the Jet Propulsion Laboratory, California Institute of Technology under a contract with NASA. This research was supported by ESTEC Contract No. 4000106398/12/NL/KML. This work was supported by the Hungarian Research Fund OTKA grants K81966 and K101393. This research has made use of the VizieR catalogue access tool, CDS, Strasbourg, France. The original description of the VizieR service was published in A&AS 143, 23.

Table 2. UKIDSS sources classified as candidate YSOs

UGPS	J	H	K_s	[3.6]	[4.5]	SST GLMC	Note
J052524.85+345800.3	17.590±0.021	16.529±0.015	15.720±0.020	14.826±0.056	14.281±0.046	G172.6121-00.3464	
J052525.94+345631.7	17.306±0.016	16.474±0.014	15.875±0.023	15.166±0.065	14.983±0.063	G172.6346-00.3572	
J052526.60+345756.5[b]	15.258±0.003	14.078±0.002	13.127±0.002	11.965±0.032	11.494±0.029	G172.6164-00.3421	
J052528.89+345627.6	16.367±0.008	15.047±0.004	13.967±0.004	13.031±0.048	12.465±0.036	G172.6412-00.3494	
J052529.76+345728.1	16.181±0.007	15.414±0.006	14.939±0.010	14.542±0.049	14.290±0.052	G172.6290-00.3376	
J052530.87+345744.5	15.992±0.006	15.198±0.005	14.656±0.008	14.065±0.054	13.884±0.041	G172.6273-00.3319	
J052532.03+345736.7	16.497±0.008	15.314±0.005	14.416±0.006	13.357±0.049	12.838±0.047	G172.6314-00.3298	
J052532.08+345721.8	17.016±0.013	16.269±0.012	15.723±0.020	14.891±0.060	14.426±0.053	G172.6349-00.3320	
J052532.08+345718.4	16.558±0.009	15.775±0.008	15.269±0.013	14.859±0.064	14.763±0.085	G172.6356-00.3325	
J052532.12+345734.7	17.197±0.015	16.223±0.012	15.549±0.017	15.007±0.104	···	G172.6320-00.3299	
J052532.51+345718.0	13.918±0.002	12.878±0.001	12.105±0.001	11.000±0.043	10.042±0.030	G172.6366-00.3313	L1516-Ha 3
J052532.60+345751.9	18.132±0.033	16.336±0.013	14.535±0.007	13.048±0.045	12.406±0.033	G172.6289-00.3258	
J052532.73+345710.7	13.125±0.001	12.162±0.001	11.544±0.001	10.641±0.058	10.217±0.035	G172.6386-00.3319	L1516-Ha 4
J052532.74+345742.6[b]	16.038±0.006	14.609±0.003	13.516±0.003	12.154±0.047	11.600±0.031	G172.6314-00.3269	
J052533.03+345648.2	15.858±0.005	14.740±0.003	13.974±0.005	12.636±0.044	12.072±0.035	G172.6444-00.3345	
J052533.85+345752.1	16.598±0.009	15.745±0.008	15.144±0.012	14.266±0.053	13.806±0.042	G172.6313-00.3222	
J052534.08+345746.6	15.062±0.003	14.122±0.002	13.561±0.003	12.894±0.036	12.405±0.039	G172.6330-00.3225	L1516-Ha 6
J052536.40+345631.1	18.169±0.035	16.926±0.021	16.041±0.026	15.328±0.068	14.899±0.067	G172.6548-00.3277	
J052537.27+345734.7	16.165±0.007	15.406±0.006	14.862±0.009	13.980±0.039	13.521±0.043	G172.6418-00.3153	
J052538.17+345635.5	17.281±0.016	16.331±0.013	15.534±0.017	14.469±0.050	13.861±0.050	G172.6572-00.3220	
J052538.69+345635.1	16.154±0.007	15.394±0.006	14.825±0.009	14.108±0.042	13.808±0.045	G172.6582-00.3205	
J052542.12+345309.8	16.718±0.010	15.092±0.004	14.077±0.005	13.006±0.047	12.462±0.029	G172.7121-00.3427	
J052543.22+345243.1	18.313±0.039	17.237±0.029	16.564±0.043	16.326±0.120	16.018±0.108	G172.7203-00.3438	
J052544.59+345357.7	17.715±0.023	16.920±0.022	16.378±0.037	15.987±0.088	15.840±0.087	G172.7057-00.3284	
J052545.12+345253.5	18.905±0.066	15.979±0.009	14.205±0.006	12.291±0.032	11.541±0.032	G172.7216-00.3368	
J052547.46+345228.3	19.162±0.083	16.984±0.023	14.953±0.010	12.970±0.054	12.323±0.039	G172.7318-00.3341	
J052548.08+345538.3	16.595±0.009	15.495±0.006	14.760±0.009	13.802±0.045	13.498±0.043	G172.6893-00.3028	
J052548.45+345101.4	16.553±0.009	15.447±0.006	14.760±0.009	14.215±0.100	14.096±0.069	G172.7537-00.3448	
J052550.09+345504.9	17.493±0.019	16.000±0.010	14.963±0.011	14.153±0.058	13.919±0.062	G172.7008-00.3023	
J052551.33+345226.6[a]	17.463±0.019	15.697±0.007	14.410±0.007	···	···	···	
J052552.02+345808.2[a,b]	14.901±0.003	13.766±0.002	12.685±0.002	11.218±0.032	10.719±0.024	G172.6624-00.2683	L1516-Ha 8
J052553.87+345201.5	16.995±0.013	15.909±0.009	15.093±0.012	14.300±0.070	13.795±0.053	G172.7413-00.3141	
J052554.39+345439.2	13.628±0.001	12.496±0.001	11.558±0.001	10.500±0.027	10.006±0.030	G172.7150-00.2941	L1516-Ha 9
J052554.52+345206.2	16.215±0.007	15.403±0.006	14.917±0.010	14.405±0.073	14.294±0.085	G172.7504-00.3175	
J052555.20+345201.2	17.561±0.020	16.712±0.018	16.114±0.029	15.266±0.083	14.936±0.073	G172.7529-00.3164	
J052556.88+345144.2	13.530±0.001	12.649±0.001	11.899±0.001	10.973±0.038	10.438±0.027	G172.7600-00.3143[c]	L1516-Ha 11
J052556.97+345018.9	16.619±0.009	15.775±0.008	15.169±0.013	14.149±0.046	13.745±0.042	G172.7798-00.3273	
J052600.97+345143.2	16.386±0.008	15.477±0.006	14.907±0.010	14.229±0.057	13.905±0.047	G172.7681-00.3029	
J052602.74+345109.3	16.000±0.006	15.014±0.004	14.377±0.007	13.386±0.039	12.901±0.037	G172.7792-00.3031	L1516-Ha 12
J052608.38+345006.3	17.028±0.014	16.277±0.013	15.754±0.022	15.125±0.054	14.860±0.062	G172.8046-00.2969	
J052613.27+344936.1	14.817±0.003	13.940±0.002	13.396±0.003	12.501±0.047	12.137±0.038	G172.8209-00.2877	
J052613.58+345316.0[a]	17.950±0.030	16.698±0.019	15.664±0.021	···	14.249±0.108	G172.7708-00.2527	
J052613.92+345329.4[a]	16.387±0.008	14.786±0.004	13.660±0.004	12.865±0.043	12.401±0.037	G172.7684-00.2496	
J052614.68+345005.2	15.802±0.005	14.870±0.004	14.320±0.006	15.125±0.054	14.860±0.062	G172.8046-00.2969	L1516-Ha 14
J052616.07+345320.0[a]	15.719±0.005	14.662±0.003	13.608±0.004	12.169±0.050	11.570±0.035	G172.7747-00.2449[c]	
J052616.37+345333.2[a]	13.410±0.001	11.948±0.001	10.781±0.001	9.053±0.080	8.284±0.042	G172.7722-00.2421	L1516-Ha 15
J052616.80+345422.3	15.500±0.004	14.657±0.003	14.031±0.005	13.247±0.045	12.784±0.030	G172.7617-00.2332	L1516-Ha 16
J052619.57+344929.5	16.103±0.007	15.180±0.005	14.621±0.008	···	15.797±0.089	G172.7826-00.2363	

Table 3. Spitzer sources classified as candidate YSOs

UGPS	J	H	K_s	[3.6]	[4.5]	SST GLMC	Note
J052527.87+345741.9	14.983±0.003	14.150±0.002	13.679±0.004	13.158±0.045	12.914±0.038	G172.6222-00.3407	L1516-Ha 1
J052529.63+345755.1	14.591±0.002	13.700±0.002	13.181±0.002	12.729±0.034	12.464±0.030	G172.6225-00.3337	L1516-Ha 2
J052529.74+345655.8	15.004±0.003	14.117±0.002	13.719±0.004	13.242±0.033	12.997±0.043	G172.6364-00.3426	
J052534.55+345800.3	16.121±0.006	15.373±0.006	14.929±0.010	14.328±0.057	14.036±0.049	G172.6308-00.3190	
J052534.98+345701.1	16.505±0.009	15.641±0.007	15.301±0.014	14.874±0.070	14.566±0.065	G172.6452-00.3270	
J052543.31+345307.2	18.492±0.045	16.860±0.021	15.983±0.026	14.754±0.060	14.364±0.057	G172.7150-00.3398	
J052544.56+345017.8	14.758±0.003	13.827±0.002	13.439±0.003	12.919±0.040	12.336±0.031	G172.7563-00.3626	L1516-Ha 7
J052546.99+345244.3	···	17.018±0.024	14.569±0.008	12.425±0.048	11.374±0.040	G172.7272-00.3329	
J052547.76+344950.9[a]	···	17.096±0.025	14.320±0.006	11.993±0.065	10.761±0.037	G172.7687-00.3577	
J052555.37+345441.9	15.465±0.004	14.447±0.003	13.869±0.004	13.030±0.038	12.673±0.036	G172.7162-00.2909	L1516-Ha 10
J052600.91+345413.1	15.949±0.006	14.974±0.004	14.549±0.008	13.633±0.044	13.173±0.038	G172.7334-00.2797	
J052601.71+344933.5	16.706±0.010	15.898±0.009	15.473±0.017	14.961±0.055	14.604±0.050	G172.7993-00.3209	
J052607.10+345425.9	14.791±0.003	13.959±0.002	13.505±0.003	12.916±0.045	12.544±0.036	G172.7423-00.2601	L1516-Ha 13
J052611.65+344904.5	16.640±0.010	15.909±0.009	15.479±0.018	14.580±0.056	14.202±0.041	G172.8250-00.2972	
J052618.28+344716.9	15.480±0.004	14.666±0.003	14.198±0.006	13.557±0.038	13.130±0.033	G172.8625-00.2951	
J052619.46+344943.9	15.410±0.004	14.501±0.003	14.045±0.005	13.392±0.048	13.079±0.038	G172.8309-00.2689	
J052619.67+344923.7	16.267±0.007	15.405±0.006	14.956±0.011	14.465±0.065	14.035±0.041	G172.8359-00.2715	

[a]Classified as a candidate galaxy in UKIDSS.

REFERENCES

Arimatsu K., Doi Y., Wada T., Takita S., Kawada M., Matsuura S., Ootsubo T., Kataza H., 2014, PASJ, 66, 47

Audard M., et al., 2014, Protostars and Planets VI, pp 387–410

Baraffe I., Homeier D., Allard F., Chabrier G., 2015, A&A, 577, A42

Barentsen G., et al., 2011, MNRAS, 415, 103

Barentsen G., et al., 2014, MNRAS, 444, 3230

Barrado y Navascués D., Martín E. L., 2003, AJ, 126, 2997

Bell C. P. M., Rees J. M., Naylor T., Mayne N. J., Jeffries R. D., Mamajek E. E., Rowe J., 2014, MNRAS, 445, 3496

Camargo D., Bonatto C., Bica E., 2012, MNRAS, 423, 1940

Camargo D., Bica E., Bonatto C., 2013, MNRAS, 432, 3349

Cardelli J. A., Clayton G. C., Mathis J. S., 1989, ApJ, 345, 245

Churchwell E., et al., 2009, PASP, 121, 213

Cutri R. M., et al., 2003, VizieR Online Data Catalog, 2246

Dewangan L. K., Ojha D. K., Luna A., Anandarao B. G., Ninan J. P., Mallick K. K., Mayya Y. D., 2016, ApJ, 819, 66

Drew J. E., et al., 2005, MNRAS, 362, 753

Fazio G. G., et al., 2004, ApJS, 154, 10

Froebrich D., Scholz A., Raftery C. L., 2007, MNRAS, 374, 399

Green G. M., et al., 2015, ApJ, 810, 25

Gutermuth R. A., Megeath S. T., Myers P. C., Allen L. E., Pipher J. L., Fazio G. G., 2009, ApJS, 184, 18

Hartmann L., Kenyon S. J., 1996, ARA&A, 34, 207

Herbig G. H., 1966, Vistas in Astronomy, 8, 109

Herbig G. H., 1977, ApJ, 217, 693

Humphreys R. M., 1978, ApJS, 38, 309

Kawamura A., Onishi T., Yonekura Y., Dobashi K., Mizuno A., Ogawa H., Fukui Y., 1998, ApJS, 117, 387

Lada C. J., 1991, in Lada C. J., Kylafis N. D., eds, NATO Advanced Science Institutes (ASI) Series C Vol. 342, The Physics of Star Formation and Early Stellar Evolution. p. 329

Lucas P. W., et al., 2008, MNRAS, 391, 136

Lynds B. T., 1962, ApJS, 7, 1

Manoj P., Bhatt H. C., Maheswar G., Muneer S., 2006, ApJ, 653, 657

Marco A., Negueruela I., 2016, MNRAS, 459, 880

Marton G., Tóth L. V., Paladini R., Kun M., Zahorecz S., McGehee P., Kiss C., 2016a, MNRAS, 458, 3479

Marton G., Tóth L. V., Paladini R., Kun M., Zahorecz S., McGehee P., Kiss C., 2016b, VizieR Online Data Catalog, 745

Meyer M. R., Calvet N., Hillenbrand L. A., 1997, AJ, 114, 288

Reipurth B., Yan C.-H., 2008, Handbook of Star Forming Regions, Volume I, ed. B. Reipurth, Astron. Soc. Pacific, p. 869

Samus N., 2009, Central Bureau Electronic Telegrams, 1896

Semkov E. H., Peneva S. P., Munari U., Dennefeld M., Mito H., Dimitrov D. P., Ibryamov S., Stoyanov K. A., 2013, A&A, 556, A60

Straižys V., Drew J. E., Laugalys V., 2010, Baltic Astronomy, 19, 169

Szegedi-Elek E., Kun M., Reipurth B., Pál A., Balázs L. G., Willman M., 2013, ApJS, 208, 28

Tognelli E., Prada Moroni P. G., Degl'Innocenti S., 2011, A&A, 533, A109

Tóth L. V., et al., 2014, PASJ, 66, 17

Werner M. W., et al., 2004, ApJS, 154, 1

Witham A. R., Knigge C., Drew J. E., Greimel R., Steeghs D., Gänsicke B. T., Groot P. J., Mampaso A., 2008, MNRAS, 384, 1277

This paper has been typeset from a TEX/LATEX file prepared by the author.